2014-07-30

Remote Sensing Applications of Ambient Noise

Geoffrey J. Banker
University of Miami, gjb2107@gmail.com

UNIVERSITY OF MIAMI

REMOTE SENSING APPLICATIONS OF AMBIENT NOISE

By

Geoffrey J. Banker

A THESIS

Submitted to the Faculty
of the University of Miami
in partial fulfillment of the requirements for
the degree of Master of Science

Coral Gables, Florida

August 2014

UNIVERSITY OF MIAMI

A thesis submitted in partial fulfillment of
the requirements for the degree of
Master of Science

REMOTE SENSING APPLICATIONS OF AMBIENT NOISE

Geoffrey J. Banker

Approved:

_____ Mike Brown, Ph.D. Professor of Applied Marine Physics	_____ Harry Deferrari, Ph.D. Professor of Applied Marine Physics
_____ Arthur Mariano, Ph.D. Professor of Meteorology and Physical Oceanography	_____ M. Brian Blake, Ph.D. Dean of the Graduate School

BANKER, GEOFFREY (M.S., Applied Marine Physics)
Remote Sensing Applications of Ambient Noise (August 2014)

This thesis supervised by Professor Michael G. Brown
No. of pages in text. (30)

It is shown that a transient Green's function can be obtained through correlations of concurrent recordings of a diffuse acoustic ambient noise field at two locations. A discussion of the history, motivation, and mathematical background of this method, "noise interferometry", is presented. The idea is demonstrated through modelling and tested using field measurements collected in December 2012 near the Florida Keys. The field experiment made use of concurrent ambient noise recordings at three locations using moored receivers placed near the bottom. The focus here is on a receiver pair separated horizontally by approximately 5 km, with the goal of showing that the estimated Green's function is suitable for tomographic inversion. In agreement with expectations based on theory, it is shown that by summing many realizations of the correlation function an approximation to the Green's function can be retrieved. The estimated Green's function is favorably compared with simulations performed with the MMPE acoustic model.

Table of Contents

Chapter 1 Introduction

This thesis will describe a method for retrieving valuable acoustic information from the ambient acoustic field, demonstrate it through modeling, and show it in results of a field experiment conducted off the Florida coast. The desired goal is to reproduce data that could be used as the foundation for tomographic measurements without the use of a mechanical source. In particular I will concern myself with a signal processing technique that has come to be referred to as noise interferometry. In this method concurrent recordings of ambient noise at two locations are correlated, and the information retrieved is an approximation of the case in which one receiver is a source. This approximation is valuable because it allows us to obtain a response at one location due to a pulse at another (deterministic Green's function) without actually creating the source pulse . With this Green's function in hand, the methods of tomographic inversion that have been well refined over the past few decades can be used to produce valuable ocean structure data. Noise interferometry offers several advantages over traditional active source methods, as will be discussed in further detail later, but in general it allows for simpler and more cost effective experiments, and eliminates the potential problems arising from the effects of active sources on marine mammals.

With the theory behind noise interferometry becoming well accepted, the approach taken here is concerned with investigating the method's actual efficacy both through models as well as in practice through a simple field experiment. The modelling approach began as a way to crudely show that a sum of correlations could indeed result in a Green's function, but as progress was made a move was made to more complex and accurate models. There were two primary models used, one ray based

and the other a parabolic equation model. The advantages and different uses of these models will be discussed later. The field-work consisted of a simple deployment of three hydrophones off of the Florida Keys. This experiment was designed to demonstrate noise interferometry as a feasible method of remote sensing in the most elementary manner possible. The goal of both the modelling and the field-work was not to conduct a complete tomographic inversion and make specific ocean structure observations, but rather simply to demonstrate that the Green's function necessary to do so can indeed be reproduced over significant distance (up to 10km) from ambient noise alone.

The remainder of the thesis is broken down into sections as follows. Section 2 provides a background of acoustic remote sensing and an overview of noise interferometry, including both a mathematical description and a discussion of its benefits and drawbacks. Section 3 describes modelling in a homogenous ocean environment, along with the use of a ray-based model to recreate an ambient acoustic field. Section 4 will present the findings of the hydrophone deployment. Section 5 will show the results of using the MMPE model to corroborate the field data, and also contrasts the ray-based and PE-based approaches. Lastly, section 6 will be a final discussion on the results and future work.

Chapter 2 Background

2.1 Ocean Acoustic Remote Sensing

Beginning in the 1980's it has been suggested that acoustic remote sensing, specifically tomography and thermometry, could be the primary means of observing large scale ocean structure (Munk and Wunsch 1982). Similarly, it has been suggested that altimetry data from satellites could also be used as the primary means of observing large scale ocean surface features. Acoustic remote sensing can be broken down into two major categories, active and passive, with active meaning a source is used, and passive meaning that you are simply listening. The primary forms of active acoustics have been the use of active sonar for bathymetry, topography, and military purposes, and ocean acoustic tomography. The latter is the method that Munk and Wunsch suggested could be the predominant means of probing the ocean on a large scale. This prediction seems promising, as tomography is a proven method and offers two major inherent advantages as a remote sensing technique. First, low-frequency sound can travel over great distances with little attenuation in the ocean. While the oceans are nearly opaque to electromagnetic waves, they are an excellent medium for low-frequency acoustic signals and therefore allow for measurement on a scale that other methods cannot achieve. Second, tomography by nature averages over the smaller temperature fluctuations in the ocean, allowing for measurements on a large scale without the interference of of small scale variability. While the potential of satellite data has largely been realized and is now common practice, and despite the benefits offered by ocean acoustic tomography, the implementation of acoustic remote sensing methods has unfortunately been limited.

While a handful of major experiments have been carried out (ATOC, SYNOP, etc…), acoustic tomography has fallen well short of the widespread application predicted by Munk and Wunsch.

The reasons for the lack of progress in the field are numerous but the most significant are the cost of the equipment (both in terms of money as well as power), the physical challenges of deploying the needed equipment, the signal processing expertise required, and the potential harm to marine mammals. All of these drawbacks arise from the use of low-frequency acoustic sources. These sources are necessarily large in order to generate the long travelling low-frequency signal required for tomography, making them difficult to deploy and operate. The sources are comparatively inefficient and therefore require large expensive power sources for any long term study. To add to the growing cost, extremely precise timing is needed and thus highly accurate clocks also become a necessity. To complicate matters further, the technical expertise required to perform the necessary signal processing is non-trivial, and demands an in-depth understanding of the use of complex pulses such as m-sequence. Lastly, concern that such sources pose a threat to marine life has led to the need for permits and complications when deploying acoustic sources. While low-frequency acoustic sources pose many challenges, acoustic receivers are comparatively simple. Hydrophones are significantly smaller and compact, making them far easier to deploy. They have low power requirements, making long term deployments a simpler possibility. There are no complicated pulse sequences involved without the use of a source so signal processing is more straightforward. Receivers are also comparatively inexpensive, making frequent use simpler and more feasible.

While the complications arising from the use of acoustic sources have deterred use of acoustic remote sensing, the observational potential of tomographic methods is too large to ignore. Here it is suggested that the same observations could be made using only the ambient acoustic field. This offers several obvious advantages. Without an acoustic source there is no threat to marine mammals; any proposed experiment is thus less complicated. Without the complex pulses used by the mechanical sources the detailed knowledge of m-sequences is no longer a necessity for signal processing. The experiment would become both financially and physically more reasonable as the hydrophones are inexpensive, energy efficient, and simpler to deploy.

The use of ambient noise as an observational tool is not in itself a revolutionary concept, as the use of “acoustic daylight” has been suggested as an imaging tool to replace methods such as active sonar. In fact, even the methods discussed here have been used successfully in seismic studies (Campillo and Paul, 2003; Picozzi et al., 2009; Shapiro et al., 2005) including helioseismology (Duvall et al., 1993; Rickett and Claerbout, 1999). Bathymetric sounding and probing of the ocean bottom have also been achieved using the ambient noise generated at the ocean surface, through the use of a vertical hydrophone array (Gerstoft et al., 2007). This last example, while similar to our work, is concerned entirely with the vertically propagating sound, while the methods discussed here are interested in the horizontally propagating sound. Given the proven success in other fields, it seems reasonable to suggest that the future of ocean acoustic remote sensing lies with the methods discussed here.

2.2 “Noise Interferometry”

As was stated above, the idea of observing the ocean with ambient noise, or “acoustic daylight”, has been discussed in the past (Buckingham et al., 1992), but noise interferometry is an altogether different method with a different purpose. Acoustic daylight uses a noisy scattered wave field in order to image an object, while noise interferometry relies on phase coherence to probe environmental properties between receiver locations. The idea that a diffuse field would contain valuable information about its medium stems from Rytov (1956), who showed that the deterministic Green’s function was reproduced by correlating two points of a diffuse electromagnetic field (Rytov et al. 1989). These studies were not geared towards use for remote sensing, but nevertheless showed that the Green’s functions could be determined from point measurements in a diffuse field. More recently, it was demonstrated that the deterministic Green’s function can be retrieved through noise cross-correlation (Lobkis and Weaver, 2001), which has provided the motivation for the pursuit of noise interferometry as a valuable remote sensing method. Since that time, noise interferometry has had proven success in a variety of fields. In addition to these proven successes, other applications are being explored and suggested in fields such as biomedical engineering, where it has been suggested that a similar method could be used to observe muscle properties, and in civil engineering where the application of ambient noise to detect structural weaknesses is being pursued.

At the core of the method is the cross-correlation function, C_{AB} , of concurrent recordings of the ambient acoustic signal at two locations x_A and x_B .

$$C_{AB}(t) = \int d\tau \; p(x_A, t+\tau)\, p(x_B, \tau) \qquad (1)$$

The basis of the theory is that the time derivative of this function is related to the Green's function $G(x_A, x_B, t)$ that describes propagation between x_A and x_B.

$$\frac{dC_{AB}(t)}{dt} \approx D(t) * [G(x_A, x_B, t) - G(x_B, x_A, -t)] \quad (2)$$

Where $*$ denotes a convolution, $D(t)$ is an approximate delta function, and $G(x, x_0, t)$ is the Green's function representing a response at location x due to pulse from a point source at x_0,

$$\left(\nabla^2 - \frac{1}{c^2(x)} \frac{\partial^2}{\partial t^2}\right) G(x \mid x_0, t) = -\delta(x - x_0)\delta(t) \qquad (3)$$

These results allow us to calculate an impulse response function between x_A and x_B by treating the receiver pair as if one were a source, or more accurately as if they were both transceivers. Given knowledge of the Green's function it is then possible to retrieve an accurate sound speed profile using the well developed practice of tomographic inversion. The method demonstrated in practice generates several correlation functions, $C_{AB}(t)$, which are then stacked and used to approximate the Green's function. (A derivation of Eq. (2) can be found in Appendix A)

As has been discussed, noise interferometry offers a number of advantages as a remote sensing tool, but there are also some significant drawbacks to consider. To date the most significant uses of noise interferometry have been in a seismological context, but the differences between observations on land and in the ocean are dramatic and bring to the fore some of the limitations of using noise interferometry in the ocean environment as compared to its geological and laboratory predecessors.

First, geological structures can be treated as a solid or at the very least a slowly changing environment. This allows for long correlations for each realization to be used while still maintaining coherence thereby increasing the accuracy of (approximate) Green's function being retrieved. The ocean by comparison is changing quickly, and as a consequence a longer correlation may not be likely to yield a stronger result. In short, due to the oceans more variable nature the actual Green's function is changing more rapidly than that of the solid Earth's, therefore making it more difficult to improve the signal-to-noise ratio by coherently stacking more correlation functions. Additional complications arise from the need for highly accurate clocks. Again the seismic sensors have the advantage, as they are land-based and can use very accurate synchronized GPS clocks. For ocean instrumentation each sensor must be independent, resulting in clock drift between receivers and a decrease in coherence over long intervals. Another difficulty with these observations in the ocean environment is that ocean sensors are generally in motion. Sensors in seismic noise interferometry are fixed, but it is nearly impossible to have a fixed moored hydrophone in the ocean, this results in another source of decrease in coherence between sensors. Lastly, the variations in the shear and compressional wave speeds in the Earth are large in comparison to those in the ocean and therefore the level of accuracy required is comparatively small. In the ocean the changes in sound speed are small but significant, therefore measurements in the ocean environment need a high level of accuracy in order to return a usable end result.

To date, the most significant uses of noise interferometry in the ocean (Siderius et al., 2010; Gerstoft, 2007) have been in the specific case of using a vertical array as a fathometer to probe the ocean bottom. While this represents a special

case, it is demonstrated proof that a Green's function can be recovered in the ocean environment. In closer relation to the research presented here, it has also been demonstrated that the Green's function, and indeed a sound speed profile, can also be retrieved horizontally over distances of 0.5 km and 3.5 km (Godin et al., 2011). The objective here is to demonstrate that similar measurements are possible over greater distances, 5 km and 10 km, in a coastal environment.

Chapter 3 Ray Models

3.1 Early Crude “Models”

The first step in demonstrating noise interferometry, is to consider it in the simplest possible conditions. While it can hardly be considered a true model and is probably better described as an example, it is useful to consider the flat bottom homogenous ocean case in which the only paths between receivers are the direct path and the various reflected paths. While there is little information to be gained through this process, aside from how deep the water is, it is a simple way to demonstrate and visualize the method and also to help refine some other points. The model was set up as a large circle with two receivers equidistant from the center. Then a large number of sources were created randomly both spatially and temporally to mimic the ambient noise of the ocean. To keep things simple, each source was treated as a pulse (delta function), assuming spherical spreading ($\sim \frac{1}{r}$) together with the use of image sources to treat reflection. The records at the two locations were then broken up into intervals, those were then correlated and summed to reproduce what a system response function would look like. In this simple case, the expected system response is a large pulse as the initial arrival followed by a large number of later arrivals decreasing in magnitude with number of bottom reflections, and changing phase with number of surface reflections. This means that the expected result of our stacked correlation functions should yield an approximation to the time-integral of that expected series of positive and negative pulses.

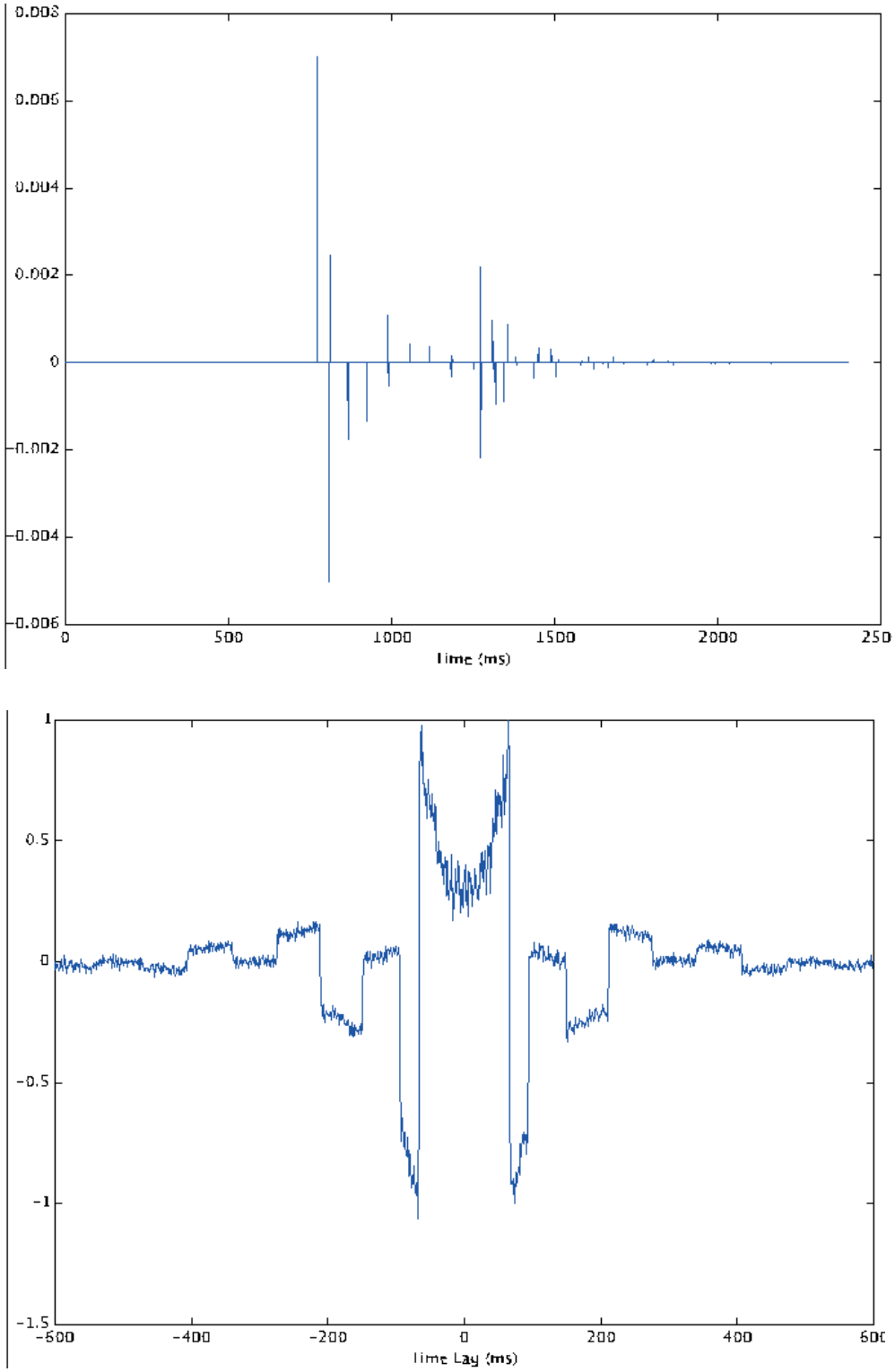

Fig. (1) Top: the expected response function at a location due to a pulse from a point source in a homogenous ocean.

Bottom: the sum of many correlation functions ($C_{AB}(t)$) in a homogenous ocean with randomly placed sources.

While the results of this crude demonstration are somewhat useful to help understand the process at work here, it was difficult to retrieve a strong signal due to the computational restraint on the number of sources. The limitations of this example are that it became computationally difficult to 1) create the number of sources needed to accurately mimic ambient noise, and 2) generate a time series long enough to include the needed number of correlations to stack. The resulting correlation function is far from noise free, but it succeeds in its simple goal of demonstrating the process of noise interferometry as a method and shows that it can work horizontally in the simplest possible environment.

3.2 Mach1 Model

While the earlier example is useful to visualize the process of noise interferometry, it is not at all an accurate representation of an actual ocean environment. In order to create a more accurate picture, we turned to using a more sophisticated model. The Mach1 model is a ray-based sound propagation model. What makes the Mach1 model particularly useful is that it performs all of its steps in the time domain, keeping the phase information intact and enabling us to use its results for our correlation. To begin, a field of random point sources was created in similar fashion to the previous example. Using an empirically obtained sound speed profile, Mach1 then computes the response (Green's function) from each source to each receiver. Through this process, we attempt to mimic an ambient acoustic field more accurately and retrieve a Green's function as we would in an actual ocean environment. After conducting many iterations of this simulated experiment, it became clear that while the resulting correlations became clearer with greater stacking times, the number of sources

needed to effectively mimic an ambient noise field made for a long run time for the program. The end results of using the Mach1 model show that there is an emerging response function in the correlation, but the signal-to-noise ratio of the resulting sum of correlations is far from optimal.

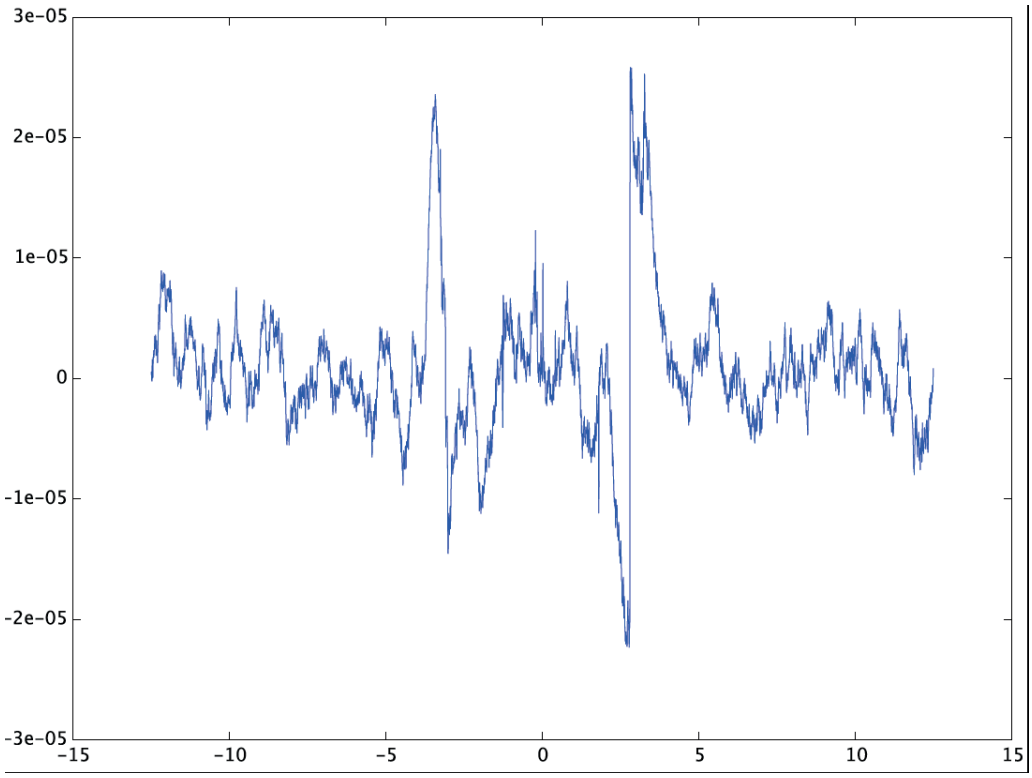

Fig. (2) Shows the stacked correlation function using values generated from the acoustic field created using the Mach1 model. The correlation is poor do to an insufficient number of sources in the field.

Chapter 4 Fieldwork

4.1 Method

On December 12 and 13, 2012 three instruments were deployed in an area about 15 km off the shore of the Florida keys. The instruments were placed inline with each other, and the area and configuration were chosen such that all three instruments were deployed very close to the 100 m isobath. All three instruments were then successfully recovered on February 12 and 13, 2013. The actual separation between receivers is 5.01 km and 9.76 km, for the 1-2 and 2-3 receiver pairs respectively. While these separations are the ones used for calculations, there is a level of inaccuracy of 10-20 m with respect to the location of each instrument. In addition to this uncertainty, the effect of the ocean bottom structure is also in question. During the deployment, several CTD casts were conducted to obtain a sound speed profile for the area.

Each instrument consisted simply of a hydrophone, recording electronics, and batteries, contained in a single housing. These instruments were based off of commercially available sensors, with the added alteration being that the standard clock was replaced with a more stable one to mitigate the previously mentioned concern of clock drift. These sensors were placed such that they were each 5 m above the bottom (~95 m depth), and recorded continuously at 8 kHz. The instrument in the middle of our deployment (Instrument 2) failed to record continuously after day six of the deployment, and so it is not possible to conduct a correlation for for a period longer than six days for either the 1-2 or the 2-3 receiver pairs. As was mentioned, due to the variability of the ocean the stacking of noise correlations over long periods of time may not actually improve the signal-to-noise ratio of the estimated Green's functions. The bulk of what is presented here will focus on the 1-2

receiver pair with some results from the 2-3 pair as well. This was chosen because the 1-2 receiver pair is the shortest separation between our instruments and therefore provides the cleanest test of our technique, while still exceeding the horizontal distance over which this method has previously been shown.

4.2 Results

As was described in section 2.2 the processing of the data obtained in this experiment consists of coherently summing many realizations of a cross-correlation function of any pair of receivers. One difficulty that was immediately apparent was the influence of other noise sources that were high in energy and non-diffusive, primarily nearby ship activity. This was dealt with initially by identifying suspiciously high energy sources and removing them from the time-sequence. Each receiver's time-sequence was then divided into sections of a length dependent upon the maximum travel time between the corresponding receiver pair, while still maximizing the number of stacked correlations for that receiver pair. One consequence of this selection is that the shorter the distance between the receiver pair is, a greater the number of correlations can be stacked. In our case the expected arrival times for the 1-2 and 2-3 receiver pairs are 3.26 s and 6.35 s, respectively, (using a sound speed profile based on CTD measurements during deployment) allowing us to use nearly twice as many correlations for the shorter instrument pair. Before stacking the correlations, each separate realization was normalized such that the maximum absolute value of each realization was equal to one. This was done to avoid some realizations dominating the end result due to the unavoidable reality that some will have inherently stronger signals. It was expected that lower frequency signals would be preferred due to higher

phase coherence and lower attenuation, and through process of trial-and-error it was found that the 50 Hz band from 20-70 Hz was a good choice of frequency band with which to perform our analysis. Above this band the correlations begin to become noisy due to higher loss of phase coherence and higher levels of attenuation which prevent the same acoustic energy from being received at both locations. Below this band (around 10 Hz and lower) the frequency response of the hydrophones is not flat and there begins to be significant bottom interaction, which is beyond the interest of this exercise.

The immediate impression that this result yields is a positive one, as the lag time at which the stacked correlation's energetic features appear is approximately the estimated travel time for the paths between receiver pairs. This is consistent with the expectation that the sum of the correlations functions is in fact an approximation to the Green's function. Another anticipated outcome is that the resulting correlation should be symmetric. It follows from equation (1) that $C_{AB}(t)$ should be an even function, and while having a perfectly homogenous source distribution is unreasonable to expect, there is also no anticipated reason to have a significantly biased acoustic field at our deployment site either. To test this result it is necessary to correct for some clock errors. There is a pre-deployment error of approximately -40 ms for the 1-2 receiver pair due to a difference in the time of activation, as well as an error during the course of the deployment due to clock drift of -2.2 ms for the 1-2 receiver pair, and +4.5 ms for the 2-3 receiver pair. These latter clock errors are relative to a time set by a pulse sent simultaneously to each instrument before deployment. The total clock error of -42.2 ms for the 1-2 receiver pair is doubled by the correlation meaning the effective time correction ~85 ms. With this correction in place, overlapping the

positive and negative lags of the correlation (Fig. 3b) does suggest that $C_{AB}(t)$ is indeed an even function, further strengthening the initial hypothesis. The initial interpretation of the results is that the stacked correlations seem consistent with the expected qualities of $C_{AB}(t)$, in particular evenness and expected multipath arrival times, and appear to be in agreement with the original hypothesis that the Green's function can indeed be retrieved through ambient noise.

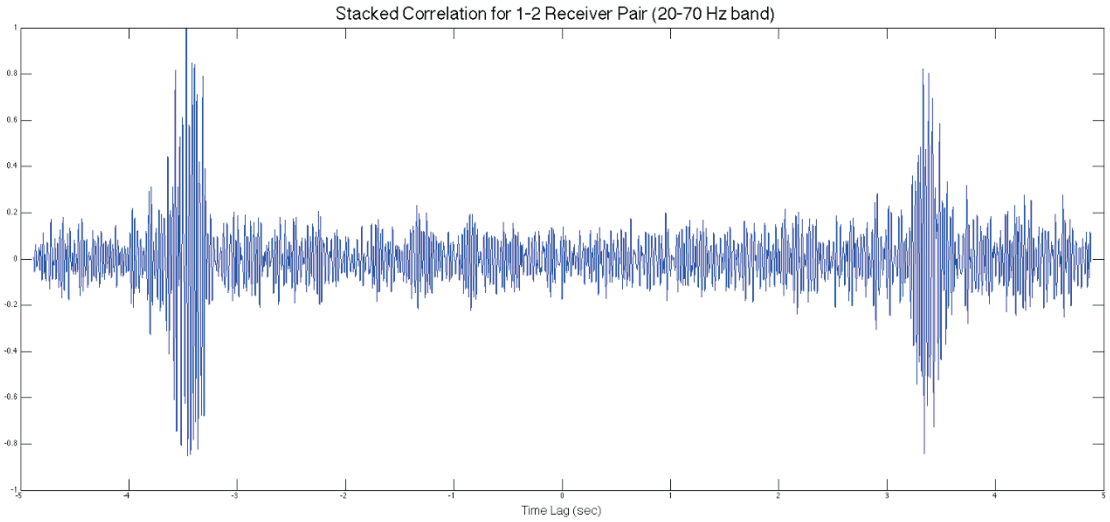

Fig. (3a) Total stacked correlation function in 20-70 Hz frequency band, stacked over approximately 6 days.

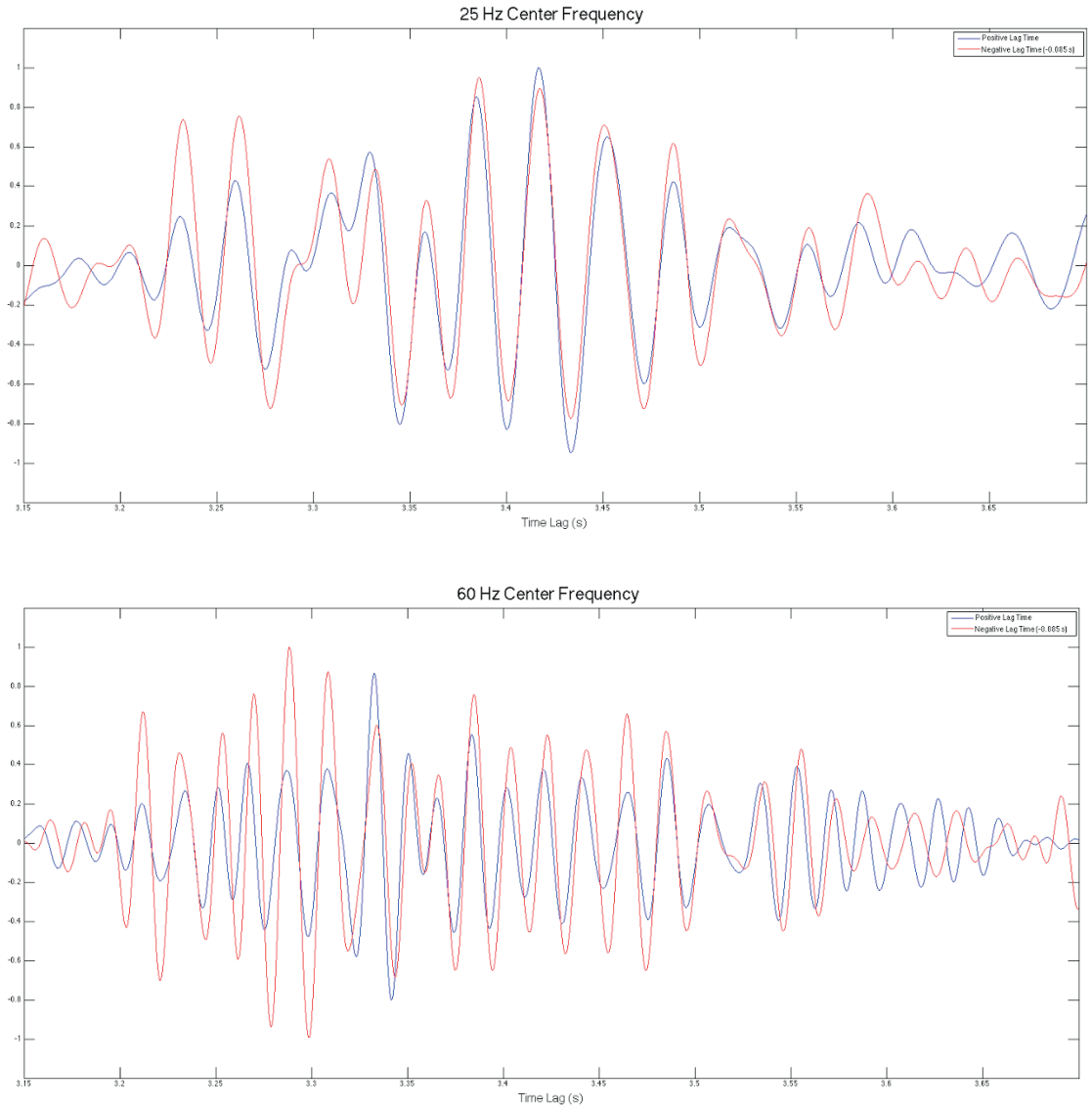

Fig. (3b) Shows stacked correlations for the 1-2 receiver pair (5.01 km separation) at the 25 Hz (top) and 60 Hz (bottom) center frequency bands. With the applied 0.085 sec time correction for synchronization discrepancy and clock drift, the positive time lag (blue line) and negative time lag (red line) of the correlation are approximately symmetric.

Chapter 5 Corollary Analysis with PE Model

5.1 MMPE Model

Monterey-Miami Parabolic Equation (MMPE) is a model for solving the parabolic form of the acoustic wave equation developed by Kevin Smith and Fred Tappert using the Split-Step Fourier Method. Using this method, the model solves the equation in small range steps, continually Fourier transforming back and forth between depth and the vertical wavenumber domain. Through this method MMPE produces an approximate numerical solution to the acoustic wave equation. The MMPE model was chosen because of its ease of use, familiarity, and most importantly its ability to give a quick, accurate result in a specific frequency band given only basic environmental information. MMPE also offers some advantages over a ray-based model. First, a ray-based model is based on a high frequency approximation, while the PE model is a full wave model that naturally accounts for diffraction. Second, the stacked correlations show some indications of a predominance of energy with low mode numbers, and MMPE is better suited to identifying modal dispersion than a ray-based model. While the MMPE model is useful and effective, its post-processing codes were not intended to create the exact output needed to compare to our field data. MMPE's codes are structured to return transmission loss at a particular depth or range. Our comparison requires that it be returned as a function of time at both a specific range *and* depth. So a separate simple code was written to take the raw output of the primary MMPE code and generate the desired output needed to compare with our data-driven result.

5.2 Use & Results

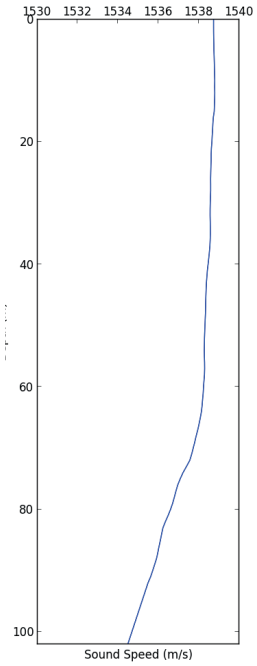

Fig. (4) Estimated sound speed profile obtained from CTD casts during the deployment and recovery cruises.

Unlike the use of the Mach1 model, the goal of using the MMPE model was not to recreate an ambient noise field, but rather to determine what an expected Green's function would look like given our conditions and instrument locations, then compare it to the processed results of the deployment. To do this, an estimated sound speed profile based on several CTD casts from both the deployment and the recovery cruises was used as seen in Fig. (4), and a reference speed of c = 1.536 km/s was used for some calculations and corrections. Other significant environmental values were input into MMPE such that the sediment layer was 10 m thick with c_b = 1.540 km/s, sound speed gradient of 1.4 1/s, density ϱ_b = 1.85 g/cm^3, and a hard bottom below with c_{db} = 2.10 km/s Consistent with the processing of the field data. The model was run in overlapping 10 Hz bands with center frequencies from 20 Hz to 70 Hz as can be seen in Fig. (5). The separate code written to achieve the desired output takes the usual three-dimensional output from MMPE, and takes only the values at the appropriate receiver depth (~95 m). In order to perform the pulse synthesis, the new code also takes into account the values at negative frequencies.

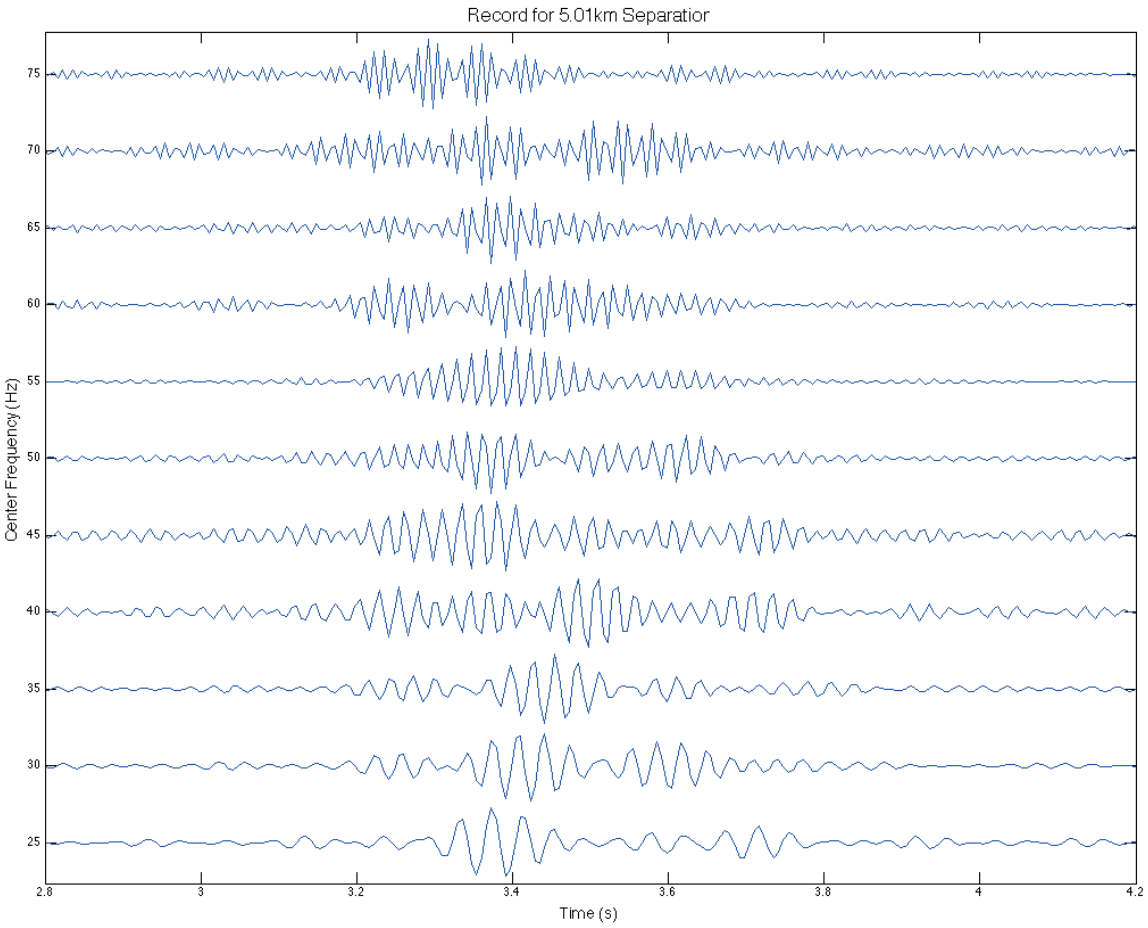

Fig. (5) Results of the MMPE model with overlapping 10 Hz bands for the 5.01 km separation.

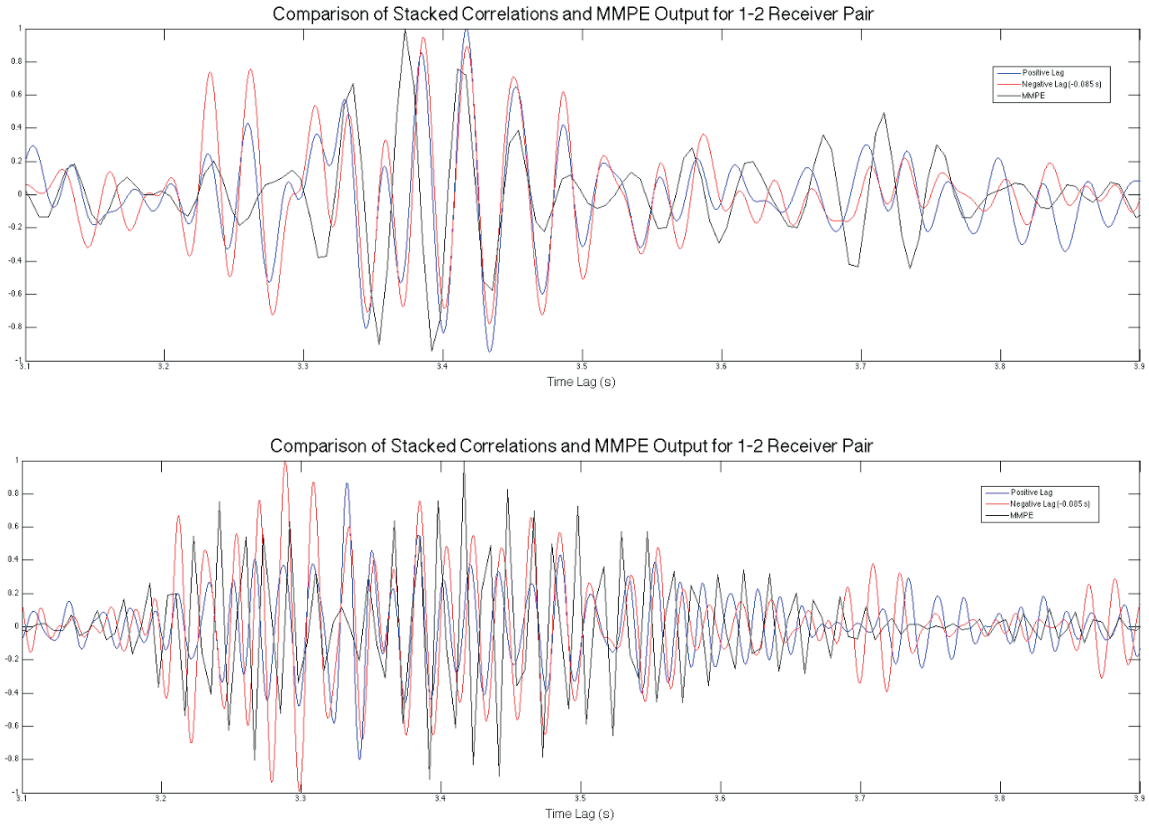

Fig. (6) Comparison of stacked correlations with MMPE predicted impulse response in the 25 Hz (top) and 60 Hz (bottom) center frequency band.

Unsurprisingly there are some differences, as the model does not consider a number of variations that exist in reality including variation of sound speed profile with range, tidal effects, any non-flat structure that may exist on the ocean bottom, and other uncertainties associated with the ocean. It is important to recall that while no model can precisely mimic the conditions of the instruments, the function resulting from the data is also itself an approximation to the actual Green's function. Despite the differences between the model and reality, and the fact that both the MMPE model and the field data generate approximations, the comparison between the impulse

response predicted by MMPE is visibly quite similar to that of the data-driven approximation (Fig. 7). In particular this relation seems to be more clearly evident at lower frequencies.

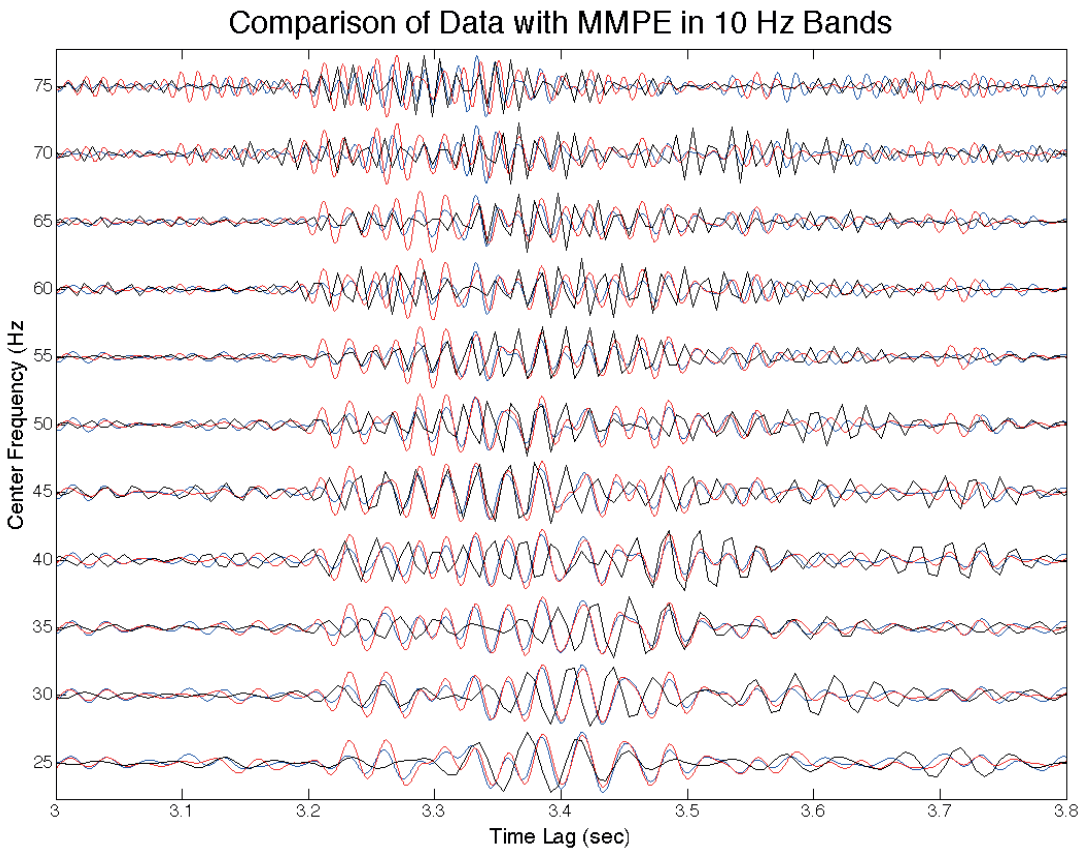

Fig. (7) Comparison of approximation from field data positive lag (blue), negative lag (red), and the MMPE result (black). Shown in overlapping 10 Hz frequency bands

Chapter 6 Summary and Discussion

The work presented here has shown that in a shallow water environment, with all of the challenges associated with the shallow water acoustic problem, that the method of noise interferometry still generates a reasonable approximation to an acoustic Green's function. These approximations are supported by agreement from calculated Green's functions obtained from the MMPE model. This success represents a departure from the previous uses of noise interferometry in the ocean, which had been either at short ranges, or specific to vertically propagating energy. The research presented does not carry through the full tomographic inversion, however it does show that measurement of ambient noise, even in challenging conditions, can result in the foundation for such inversions.

The deployment discussed here demonstrated that the method of noise interferometry can be used to retrieve the Green's function from two simultaneous ambient noise recordings, and therefore is a viable tool for remote sensing. The conditions of the experiment, however, were less than ideal and another deployment was conducted in August-September of 2013 to obtain more data. The major issues with the first deployment were that, the instruments were deployed in a very shallow setting (<100 m), the time of year affected the temperature profile, and the failure of instrument two limited the amount of useable data collected. The depth and temperature profile issues go hand in hand in that at that time of year (December-February) the temperature profile changes little with depth down to 100m, while exhibiting seasonal cooling over the course of the experiment. The shallow nature of the experiments is also a significant drawback, as shallow water acoustic propagation is generally more complicated than in deep water. The failure of

instrument two after the sixth day of the deployment limited the amount of data to use in stacking the correlations, but it is unclear how much additional stacking time would have aided in the end result. The second deployment seeks to mitigate some of these issues by deploying in deeper water (>600 m) and under better seasonal conditions. This of course brings other concerns, such as high current, inconsistent receiver depths, and more highly varying seafloor structure.

Both deployments address the same goal, to demonstrate that the Green's function can be retrieved from two concurrent recordings of ambient noise. While these results are of great use and importance, it is the first step towards being able to use noise interferometry as an effective means of acoustic remote sensing. The next step is to use the information similar to that obtained through the stacked correlations presented here to retrieve the sound speed profile. This has in fact been done over distances up 3.5 km (Godin et al., 2011). Moving forward, in order to be a more useful tool for probing the oceans in the manner that Munk and Wunsch suggested active tomography could be used, that result will have to be demonstrated at much greater distances. The results discussed here show that a Green's function can be acquired between receivers with a 10 km separation in shallow non-ideal conditions, and it is therefore not unreasonable to suggest that a similarly constructed experiment in deep water would result in successful Green's function retrieval over much greater distances.

Appendix

The material presented here closely follows the material in an unpublished note by Brown (2013).

Beginning with the equation for acoustic pressure, for a point source at x_0 with time history $s(t)$,

$$\left(\nabla^2 - \frac{1}{C^2(x)}\frac{\partial^2}{dt^2}\right) p(x \mid x_0,\ t) \ = \ -s(t)\ \delta(x - x_0)$$

The solution can be written as $p(x \mid x_0,\ t) \ = \ s(t) \ * \ G(x \mid x_0,\ t)$ where $G(x \mid x_0,\ t)$ is the Green's function which satisfies

$$\left(\nabla^2 - \frac{1}{c^2(x)}\ \frac{\partial^2}{\partial t^2}\right) G(x \mid x_0,\ t) \ = \ -\delta(x - x_0)\delta(t) \qquad (2a)$$

In the frequency domain as $p'(x \mid x_0,\ \omega) \ = \ s'(\omega)\ G'(x \mid x_0,\ \omega)$ where $G'(x \mid x_0,\ \omega)$ satisfies

$$(\nabla^2 + k^2(x))\ G'(x \mid x_0,\ \omega) \ = \ -\delta(x - x_0) \qquad (2b)$$

and $k^2(x) \ = \ \omega^2/c^2(x)$.

Considering a random distribution of point sources at positions x_i with time histories $s_i(t),\ p(x_A \mid x_i,\ t) \ = \ s_i(t) \ * \ G(x_A \mid x_i,\ t)$ is the acoustic pressure at x_A from a source at x_i. A similar equation can be written for x_B and x_j. Summing the contributions from each of the random sources for both A and B, and then cross-correlating the now summed acoustic pressure records yields

$$C_{AB}(t) \ = \ \sum_i p(x_A \mid x_i,\ t) \ * \sum_j p(x_B \mid x_j,\ -t)$$

$$= \sum_i \sum_j s_i(t) * G(x_A \mid x_i, t) * s_j(-t) * G(x_B \mid x_i, -t)$$

$$C_{AB}(t) = D(t) * \sum_i G(x_A \mid x_i, t) * G(x_B \mid x_i, -t)$$

Where $D(t)$ has been defined by $s_i(t) * s_j(-t) = \delta_{ij} D(t)$, with the assumption that the randomly distributed sources are independent with autocorrelation functions that approximate delta functions. If we now consider the distribution of sources to be continuous, then this equation becomes

$$C_{AB}(t) = D(t) * \int\int\int dx\, G(x_A \mid x, t) * G(x_B \mid x, -t)$$

Introducing some dissipation that is proportional to $\omega \frac{\varepsilon}{2}$ our Green's functions now become

$$\left(\nabla^2 + k^2 + i\omega\varepsilon/2\right) G'(x|x_A, \omega) = -\delta(x - x_A) \qquad (A1)$$

$$\left(\nabla^2 + k^2 + i\omega\varepsilon/2\right) G'(x_B|x, \omega) = -\delta(x - x_B) \qquad (A2)$$

After multiplying Eq (A1) by $G'^*(x_B|x, \omega)$ (where the superscript * denotes complex conjugation), integrating, and complex conjugation of both sides we obtain

$$\int\int\int dx\, G'(x_B|x, \omega)\left(\nabla^2 + k^2 + i\omega\varepsilon/2\right) G'^*(x_A|x, \omega) = -G'(x_B|x_A, \omega) \qquad (A3)$$

Similarly for (A2) and $G'^*(x_A|x, \omega)$

$$\int\int\int dx\, G'^*(x_A|x, \omega)\left(\nabla^2 + k^2 + i\omega\varepsilon/2\right) G'(x_B|x, \omega) = -G'^*(x_A|x_B, \omega) \qquad (A4)$$

Eq. A3 minus Eq. A4 leaves

$$Q - i\omega\varepsilon \int\int\int dx\, G'(x_B|x, \omega) G'^*(x_A|x, \omega) = G'^*(x_A|x_B, \omega) - G'(x_B|x_A, \omega)$$

$$= \; -2\, Im\, G'(x_B|x_A,\omega)$$

Q can be written $Q = \int\int d\sigma\, [G'(x_B|x,\omega)\nabla G'^{*}(x_A|x,\omega) - G'^{*}(x_A|x,\omega)\nabla G'(x_B|x,\omega)] \cdot n$,

where n is the unit outward normal. The surface integral form of Q reveals that Q vanishes in the presence of commonly encountered boundary conditions such as rigid or pressure release boundaries.

Eliminating Q and returning to the time domain gives us

$$\varepsilon \frac{d}{dt} \int\int\int dx\, G(x_B|x,t) \; * \; G(x_A|x,-t) \; = \; G(x_B|x_A,-t) - G(x_B|x_A,t)$$

The term within the integral is equivalent to the cross-correlation function $C_{AB}(t)$, so can replace that and differentiate to eliminate the integral. When this is done we are left with the equation of primary importance to the idea of noise interferometry

$$\frac{d}{dt}[\varepsilon C_{AB}(t)] \; = \; D(t) \; * [\; G(x_B|x_A,-t) \; - \; G(x_B|x_A,t) \;]$$

References

Brooks, L.A. and Gerstoft, P (2007) Ocean Acoustic Interferometry *J. Acoust. Soc. Am* **121** 3377-3385

Brown, Michael G. (2013) Fundamentals of Acoustic Noise Interferometry *Unpublished Letter*

Brown, Michael G., O.A. Godin, N.J. Williams, N.A. Zabotin, L. Zabotina, G.J. Banker (2014) Acoustic Green's Function Extraction from Ambient Noise in a Coastal Ocean Environment. *Geophys. Res. Lett.* (Manuscript submitted for publication)

Buckingham, M. J, B.V. Berkhout, S.A.L. Glegg (1992) Imaging the Ocean with Ambient Noise. *Nature Lett.* **356** pg 327

Buckingham, M. J. (2012) Cross-Correlation in Band-Limited Ocean Ambient Noise Fields *J. Acoust. Soc. Am.* **131** 2643-2657

Campillo, M and Paul, A (2003) Long-Range Correlations in the Diffuse Seismic Coda *Science* **299** 547

Godin, O.A., N.A. Zabotin, V.V. Goncharov (2010) Ocean Tomography with Acoustic Daylight *Geophys. Res. Lett.* **37**

Godin, O. A., V.V. Goncharov, N.A. Zabotin (2012) Passive Ocean Acoustic Tomography *Doklady Earth Sciences* **444** part 1, pg 606-609

Munk, W. and Wunsch, C. (1982) Observing the Ocean in the 1990's *Phi. Trans. R. Soc. Lond.* A **307**, 439-464

Picozzi, M., Parolai, S., Bindi, D., Strollo (2009) Characterization of Shallow Geology by High-Frequency Seismic Noise Tomography *A. Geophys. J. Int.* **176** 164–174

Rickett J. and Claerbout J. (2001) Acoustic Daylight Imaging via Spectral Factorization: Helioseismology and Reservoir Monitoring *Stanford Exp. Proj., Report* 171–181

Sabra, K.G., Gerstoft, Roux, P., Kuperman W.A. (2005) Extracting Time-Domain Green's Function Estimates from Ambient Seismic Noise *Geophys. Res. Lett.* **32**

Sabra, K. G., P. Roux, W.A. Kuperman (2008) Extracting the Local Green's Function on a Horizontal Array from Ambient Noise. *J. Acoustical Society of Americ*a **124**

Schapiro, N.M., Campillo, M., Stehly, L., and Ritzwoller M.H. (2005) High Resolution Surface Wave Tomography From Ambient Seismic Noise *Science* **307** 1615-1618

Siderius, M., Gerstoft, P., Hodgkiss, W., et al. (2010) Adaptive Passive Fathometer Processing *J. Acoust. Soc. Am.* **127** 2193-2200